Investigation of LaF_3 as a vacuum ultraviolet emitter for scintillator and laser applications

Marilou Cadatal-Raduban[1,2*], Luong Viet Mui[2], Minh Hong Pham[3], Toshihiko Shimizu[2], Nobuhiko Sarukura[2], and Kohei Yamanoi[2]

[1]Centre for Theoretical Chemistry and Physics, School of Natural and Computational Sciences, Massey University, Albany, Auckland 0632 New Zealand

[2]Institute of Laser Engineering, Osaka University, 2-6 Yamadaoka, Suita, Osaka 565-0871 Japan

[3]Institute of Physics, Vietnam Academy of Science and Technology, Hanoi, Vietnam

INTRODUCTION

Scintillators are the key components in detectors used for sensing high-energy radiation. As such, scintillators are used in a wide range of scientific, industrial, and technological fields. In many applications such as those involving time-of-flight measurements and in imaging, a fast-response detector is needed. Scintillation decay time dictates the timing resolution of the radiation detector. Therefore, a scintillator with a fast scintillation decay time along with a high photon yield is required. Scintillation decay time is fundamentally related to the photoluminescence decay time of the material. The scintillation decay time is approximately proportional to the wavelength cubed, which means that a fast-response scintillator usually has a short emission wavelength [1]. Therefore, scintillators emitting in the vacuum ultraviolet (VUV) region are being investigated in order to develop fast-response scintillators. Wide band gap fluoride crystals with band gap energies greater than 6 eV has short emission wavelengths in the VUV region especially when doped with rare earth (RE) ions such as trivalent neodymium (Nd^{3+}) and erbium (Er^{3+}) [2-5]. Photoluminescence from RE-doped fluorophosphate glass scintillators, such as $20Al(PO_3)_3$-80LiF (APLF80), have also been reported to have fast nanosecond scintillation decay times and sufficient light yield for neutron detection. [6-9] Self-trapped exciton (STE) luminescence observed in undoped wide band-gap insulators such as BaF_2 [10], SrF_2 [11], CaF_2 [12] and their mixed compounds [13,14] also yield fast luminescence. In some fluoride materials such as CsF [15] and BaF_2 [10,16], cross luminescence (CL) or Auger free luminescence results to short emission wavelengths with very fast photoluminescence decay times [17]. We have previously reported the 172-nm emission from a Nd^{3+}-doped lanthanum fluoride ($Nd^{3+}LaF_3$) crystal excited by the 157-nm emission of a F_2 laser where a fast nanosecond photoluminescence decay time was observed. The photoluminescence was ascribed to allowed dipole transitions from the lowest level of the $4f^25d$ excited state configuration to the lowest ($^4I_{9/2}$) level of the $4f^3$ ground state configuration. Similar photoluminescence characteristics were observed when the crystal was excited via step-wise absorption of 290 nm (third harmonics), femtosecond pulses from a Ti:Sapphire laser. In particular, the time-resolved photoluminescence spectra for both excitations were single exponential with a decay time of about 7 ns [18,19]. When the Nd^{3+}:LaF_3 crystal was excited by the 51-nm wavelength emission of an extreme ultraviolet free-electron laser, we observed a peculiar behavior whereby the time-resolved photoluminescence spectra manifested fast and slow decay time components. As mentioned above, the fast decay component is important for scintillator applications. The origin of the double exponential photoluminescence decay time that was observed with EUV-FEL excitation is further investigated. By performing numerical simulations to reveal the electronic properties of LaF_3, the origin of the fast photoluminescence decay component is elucidated. Our results also suggest the possibility of achieving a fast decay time through CL in LaF_3.

Photoluminescence emission was obtained from a Czochralski method-grown Nd^{3+}:LaF_3 single crystal. The crystal is a cuboid with optically polished facets, each measuring 1 cm. The crystal was placed inside a vacuum chamber maintained at a pressure of 10^{-5} Pa. The sample was excited by pulses from the extreme ultraviolet free electron laser (EUV-FEL) SCSS test accelerator. The laser pulses had a wavelength of 61 nm, pulse duration of 100 fs, pulse energy of 30 μJ, and repetition rate of 30 Hz. The pulses were focused onto the crystal by ellipsoidal and cylindrical mirrors. The mirrors had a working distance of 1 m, resulting to a beam spot size of 20 μm at the surface of the crystal. Photoluminescence from Nd^{3+}:LaF_3 was collected and focused by MgF_2

lenses onto the entrance slit of a VUV Seya-Namioka spectrometer. The time-resolved photoluminescence spectrum was obtained using a VUV streak camera unit, which consisted of a holographic grating spectrometer with a groove density of 600 grooves/mm and a linear dispersion of 8 nm/mm. The effective F-number of the streak camera unit is 4.2. The detailed specifications and schematic diagrams of the spectrometer and streak camera system used in this work can be found elsewhere. [20] As a reference, the time-independent and time-resolved photoluminescence spectra of Nd^{3+}:LaF_3 under F_2 laser excitation was also obtained. The F_2 laser emission had a wavelength of 157 nm and pulse duration of 5 ns.

The absorption spectra of LaF_3 were investigated by obtaining the room-temperature absorption spectrum of LaF_3 using the solid-state spectroscopy beamline (BL7B) of the synchrotron radiation facility (UVSOR-II) at the Institute for Molecular Science in Japan. Details of the beamline can be found in the activity report of the facility. [21] The experimental band gap of LaF_3 was obtained from the absorption spectra using a Tauc plot. All measurements were performed at room temperature.

The electronic band structure of LaF_3 was calculated based on Density Functional Theory (DFT) within the generalized gradient approximation (GGA) using the Perdew-Burke-Ernzerhof (PBE) hybrid functional including exact exchange, [22, 23] where 75% PBE exchange was mixed with 25% exact exchange (PBE0). The calculations were implemented in the Vienna Ab initio Simulation Package (VASP) using plane-wave basis sets within the projector-augmented wave (PAW) method with a sufficiently high plane-wave basis cutoff of 500 eV. The valence band maxima in the band structure and DOS diagrams are shifted to zero energy.

The Green's function and screened Coulomb interaction (GW) approximation [24-27] was employed to calculate the absorption spectrum of LaF_3. This fully self-consistent quasiparticle calculation accounts for self-interaction corrections and can model excited state properties, such as absorption spectra. The changes in the exchange correlation potential are taken into account while the local field effects were neglected because microscopic changes to the periodic potential of the cell are negligible when modelling a perfect fluoride compound. [28] The absorption spectrum was extracted from the imaginary part of the frequency-dependent complex dielectric tensor, which represents the linear response of the system to an external electromagnetic field. The mathematical details for the relationship between the complex dielectric tensor and the absorption spectrum can be found elsewhere. [28]

Numerical simulations were performed to investigate the electronic properties of LaF_3 and illuminate the difference observed in the time-resolved photoluminescence spectra. Figure 1 shows the electronic band structure of LaF_3 calculated along the high symmetry lines of the first Brillouin zone. The valence band maximum and the conduction band

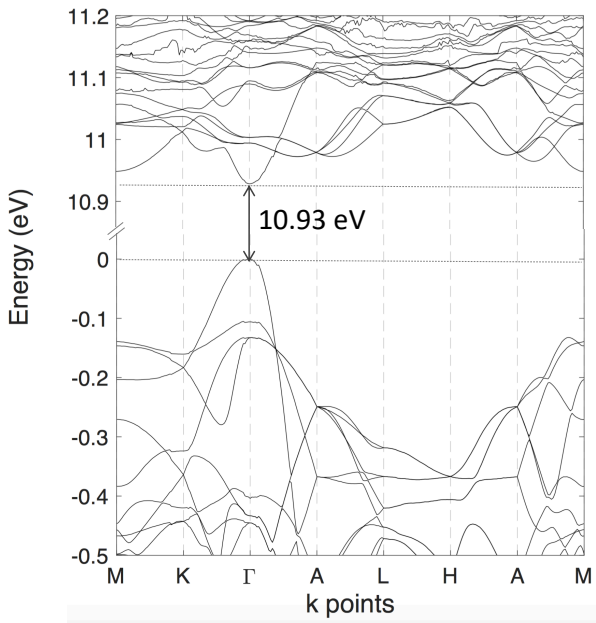

Fig. 1. Electronic band structure of LaF3 showing a direct band gap at the Γ-point of 10.93 eV.

minimum are both located at the high symmetry gamma-point. Thus, LaF_3 has a calculated direct band gap energy (Eg) of 10.9 eV. This is higher than previously reported calculated band gap energy of 7.74 eV [29] using local density approximation (LDA). It is well-known that LDA underestimate band gap energies. Previous works have demonstrated that using hybrid functionals that incorporate a fraction of nonlocal Hartree-Fock exchange leads to results that are more consistent with experiments. [27, 28, 30] The band gap energy was also calculated using the GW approximation. The band gap using GW approximation is 10.8 eV. Figure 2 shows the experimental and numerical absorption spectra of LaF_3. The experimental band gap calculated from the absorption spectra is about 10.1 eV.

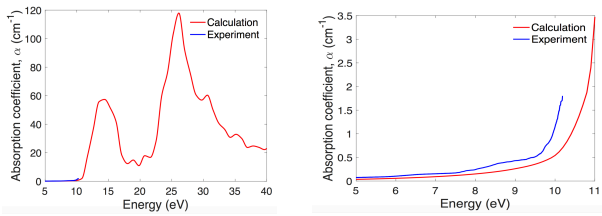

Fig. 2. Experimental and numerical absorption spectra. The figure on the right is a zoomed-in version of the figure on the left, focusing at the low energy range of the detector used in the experiment.

The density of states (DOS) of LaF_3 was calculated in order to obtain a more detailed understanding of the electronic band structure and transitions between valence and conduction bands. Figure 3 shows the DOS and site-projected DOS (PDOS) for the individual atomic contributions to the valence and conduction bands. The direct band gap transition originates predominantly from the F^- (2p) states of the valence band maximum and the La^{3+} (4f) states of the conduction band minimum. The

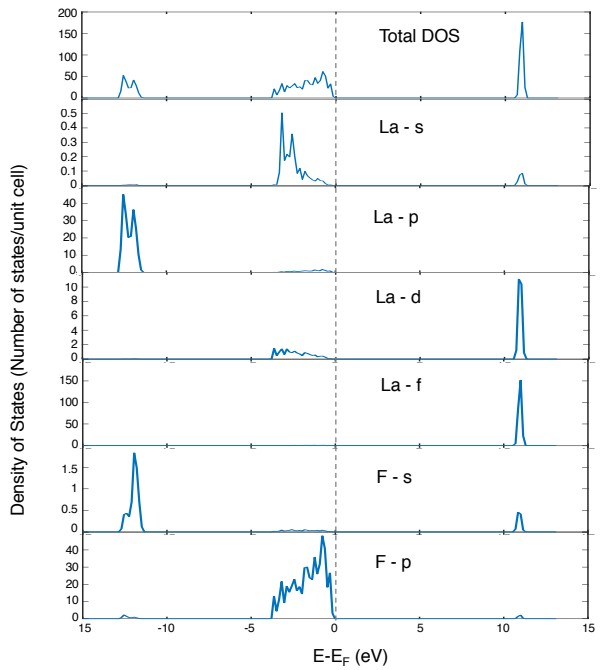

Fig. 3. DOS and PDOS for the individual atomic contributions to the valence and conduction bands.

width of the valence band is 3.5 eV. Examining the PDOS further reveals that the outermost core band originates mainly from the La^{3+} (5p) state. Therefore, the PDOS of LaF_3 alludes to the possibility of Auger-free luminescence or cross luminescence (CL). Partial CL in LaF_3 is feasible provided that the exciting photon has an energy of at least 22 eV in order to satisfy the third condition. The partial CL transition would be from the bottom of the valence band to the top of the outermost core band. The 61-nm excitation from the EUV-FEL is just enough to promote a hole from the top of the outermost core band to the bottom of the conduction band. An electron from the bottom of the valence band fills the hole in the outermost core band, resulting to the emitted CL photon with an energy of about 7.2 eV (172 nm), which corresponds to the photoluminescence emission peak observed [19]. This partial CL could account for the 1.9 ns fast decay time component observed in the time-resolved photoluminescence spectrum [19]. This also explains the faster rise time observed with EUV-FEL excitation. The slow decay time component observed in the time-resolved photoluminescence spectrum is due to the interconfigurational $4f^25d$-$4f^3$ transition in Nd^{3+}, which also explains the reason why the slow decay component is similar to the single exponential decay time obtained with the F_2 laser excitation. Interestingly, the energy difference between the bottom of the valence band and the top of the outermost core band (fast partial CL transition) is similar to the energy difference between the lowest level of the $4f^25d$ excited state configuration to the $^4I_{9/2}$ level of the $4f^3$ ground state configuration of the Nd^{3+} activator ion (slower interconfigurational transition). Therefore, only a single photoluminescence peak was observed. The schematic diagram of the electronic transitions in Nd:LaF_3 resulting to the experimentally observed double exponential decay time is shown in Figure 4. The same figure also illustrates the proposed CL mechanism in LaF_3. Experiments with undoped LaF_3 are being planned in the near future to understand the role of STE and whether the formation of STE contributes to the slow decay component. The planned experiments will also verify CL in LaF_3. The presence of CL will enhance the potential of LaF_3 as a fast-response scintillator for many applications requiring a fast, high-energy radiation detector.

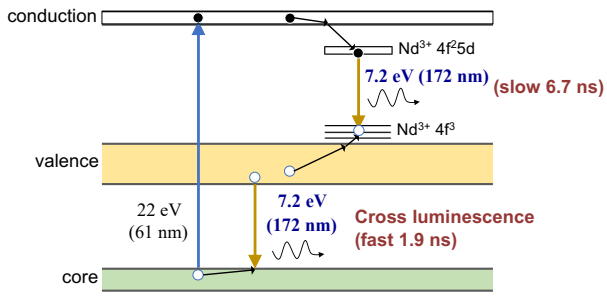

Fig. 9. Schematic diagram of the electronic transitions in Nd:LaF3 resulting to the experimentally observed double exponential decay time, and the proposed CL in LaF3.

In conclusion, we investigated the photoluminescence properties of Nd^{3+}:LaF_3 under EUV-FEL excitation. In particular, the peculiar double exponential character of the vacuum ultraviolet photoluminescence peak with a fast decay time of 1.9 ns and a slow decay time of 6.7 ns was explored to exploit the possibility of developing a fast response scintillator. The slow decay component, which is of lesser importance, is due to interconfigurational $4f^25d$-$4f^3$ transition in Nd^{3+}. Meanwhile, the electronic structure of LaF_3 obtained from first principles DFT calculations using PBE0 as implemented in VASP reveal that the fast decay component could be due to partial CL as an electron from the bottom of the valence band fills the hole in the outermost core band. The experimental and numerical results allude to the potential of LaF_3 as a fast-response scintillator, through CL, for many applications especially those relying in time-of-flight measurements.

ACKNOWLEGEMENT(S)

This research was funded by the Massey University Research Fund (MURF), the Strategic Research Excellence Fund (SREF 1000022242), The ILE and the Tohoku University Collaborative Research grant. The authors would like to thank the SCSS Test Accelerator Operation Group at RIKEN for their continuous support during this study. M. Cadatal-Raduban would like to acknowledge Mike Yap (Centre for Theoretical Chemistry and Physics, Massey University) for the technical support in using the SIMURG high performance computing cluster.

REFERENCE(S)

[1] Yanagida, T.; Fujimoto, Y.; Yamaji, A.; Kawaguchi, N.; Kamada, K.; Totsuka, D.; Fukuda, K.; Yamanoi, K.; Nishi, R.; Kurosawa S.; Shimizu, T.; Sarukura, N. Study of the correlation of scintillation decay and emission wavelength. *Rad. Meas.* **2013**, *55*, 99-102.

[2] Cadatal, M.; Furukawa, Y.; Ono, S.; Pham, M.; Estacio, E.; Nakazato, T.; Shimizu, T.; Sarukura, N.; Fukuda, K.; Suyama, T.; Yoshikawa, A.; Saito, F. Vacuum ultraviolet luminescence from a micro-pulling-down method grown Nd^{3+}:$(La_{0.9},Ba_{0.1})F_{2.9}$. *J. Lumin.* **2009**, 129, 1629-1631.

[3] Arita, R.; Minami, Y.; Cadatal-Raduban, M.; Pham, M. H.; Empizo, M. J. F.; Luong, M. V.; Hori, T.; Takabatake, M.; Fukuda, K.; Mori, K.; Yamanoi, K.; Shimizu, T.; Sarukura, N.; Fukuda, K.; Kawaguchi, N.; Yokota, Y.; Yoshikawa, A. Significant blue-shift in photoluminescence excitation spectra of Nd^{3+}:LaF_3 potential laser medium at low-temperature. *Opt. Mater.* **2015**, 47, 462-464.

[4] Cadatal-Raduban, M.; Shimizu, T.; Yamanoi, K.; Takeda, K.; Minh H. P.; Nakazato, T.; Sarukura, N.; Kawaguchi, N.; Fukuda, K.; Suyama, T.; Yanagida, T.; Yokota, Y.; Yoshikawa, A. Micro-pulling down method-grown Er^{3+}:$LiCaAlF_6$ as prospective vacuum ultraviolet laser material. *J. Cryst. Growth* **2013**, 362, 167-169.

[5] Shimizu, T.; Cadatal-Raduban, M.; Yamanoi, K.; Takatori, S.; Kouno, M.; Pham, M.; Estacio, E.; Nakazato, T.; Sarukura, N.; Kawaguchi, N.; Fukuda, K.; Suyama, T.; Yanagida, T; Yokota, Y.; Yoshikawa, A.; Saito, F. Er:LiCAF as potential vacuum ultraviolet laser material at 163 nm, *IEEE Trans. Nucl. Sci.* **2010**, 57, 1204-1207.

[6] Minami, Y.; Gabayno, J.L.; Agulto, V.C.; Lai, Y.; Empizo, M.J.F.; Shimizu, T.; Yamanoi, K.; Sarukura, N.; Yoshikawa, A.; Murata, T.; Guzik, M.; Guyot, Y.; Boulon, G.; Harrrison, J.A.; Cadatal-Raduban, M. Spectroscopic investigation of praseodymium and cerium co-doped $20Al(PO_3)_3$-80LiF glass for potential scintillator applications, *J. Non-Cryst. Solids* **2019**, 521, 119495.

[7] Empizo, M. J. F.; Cadatal-Raduban, M.; Murata, T.; Minami, Y.; Kawano, K.; Yamanoi, K.; Shimizu, T.; Sarukura, N.; Guzik, M.; Guyot, Y.; and Boulon, G. Spectroscopic properties of Pr^{3+}-doped $20Al(PO_3)_3$-80LiF glasses as potential scintillators for neutron detection, *J. Lumin*. **2018**, 193, 13-21.

[8] Watanabe, K; Arikawa, Y.; Yamanoi, K.; Cadatal-Raduban, M.; Nagai, T.; Kouno, M.; Sakai, K.; Nazakato, T.; Shimizu, T.; Sarukura, N.; Nakai, M.; Norimatsu, T.; Azechi, H.; Yoshikawa, A.; Murata, T.; Fujino, S.; Yoshida, H.; Izumi, N.; Satoh,

N.; Kan, H. Pr or Ce-doped, fast-response and low-afterglow cross-section-enhanced scintillator with 6Li for down-scattered neutron originated from laser fusion, *J. Cryst. Growth* **2013,** 362, 288-290.

[9] Yamanoi, K.; Murata, T.; Arikawa, Y.; Nakazato, T.; Cadatal-Raduban, M.; Shimizu, T.; Sarukura, N.; Nakai, M.; Norimatsu, T.; Nishimura, H.; Azechi, H.; Fujino, S.; Yoshida, H.; Yoshikawa, A.; Satoh, N.; Kan, H. Luminescence properties of Nd^{3+} and Er^{3+} doped glasses in the VUV region, *Opt. Mater*. **2013**, 35, 1962-1964.

[10] Laval, M.; Moszynski, M.; Allemand, R.; Cormoreche, E.; Guinet, P.; Odru, R. et al. Barium fluoride inorganic scintillator for subnanosecond timing, *Nucl. Instrum. Methods Phys. Res.* **1983**, 206, 169–176.

[11] Shendrik, Y.R.; Radzhabov, A.; Nepomnyashchikh, A.I. Scintillation properties of SrF_2 and SrF_2-Ce^{3+} crystals, *Tech. Phys. Lett*. **2013**, 39, 587–590.

[12] Mikhailik, V.B.; Kraus, H.; Imber, J.; Wahl, D. Scintillation properties of pure CaF_2, *Nucl. Instrum. Methods Phys. Res. A* **2006**, 566, 522–525.

[13] Yanagida, T.; Kawaguchi, N.; Fujimoto, Y.; Fukuda, K.; Watanabe, K.; Yamazaki, A. et al. Scintillation properties of LiF-SrF_2 and LiF-CaF_2 eutectic. *J. Lumin*. **2013**, 144, 212–216.

[14] Yanagida, T.; Fujimoto, Y.; Fukuda, K.; Kawaguchi, N.; Watanabe, K.; Yamazaki, A. et al. Ce-doped LiF-SrF_2 eutectic scintillators for thermal neutron detection produced at different solidification rates. *Opt. Mater*. **2013,** 35, 1449–1554.

[15] Moszynski, M.; Allemand, R.; Odru, M.L.R.; Vacher, J. Recent progress in fast timing with CsF scintillators in application to time-of-flight positron tomography in medicine. Nucl. Instrum. Methods Phys. Res. 1983, 205, 239–249.

[16] Myasnikova, A.; Radzhabov, E.; Mysovsky, A. *Ab initio* calculation of BaF_2 cross-luminescence spectrum, *J. Lumin.* **2009**, 129, 1578-1580

[17] Rodnyi, P.A.; Core-valence luminescence in scintillators, *Rad. Meas.* **2004,** 38, 343-352.

[18] Nakazato, T.; Cadatal-Raduban, M.; Yamanoi, K.; Tsuboi, M.; Furukawa, Y.; Pham, M.; Estacio, E.; Shimizu, T.; Sarukura, N.; Fukuda, K.; Suyama, T.; Yanagida, T.; Yokota, Y.; Yoshikawa, A.; Saito, F. Nd^{3+}:LaF_3 as a Step-Wise Excited Scintillator for Femtosecond Ultraviolet Pulses, *IEEE Trand. Nucl. Sci.* **2010**, 57, 1208-1210.

[19] Shinzato, Y.; Yamanoi, K.; Nishi, R.; Takeda, K.; Nakazato, T.; Shimizu,T.; Sarukura, N.; Cadatal-Raduban, M.; Fukuda, K.; Kurosawa, S.; Yokota, Y.; Yoshikawa, A.; Togashi, T.; Nagasono, M.; Ishikawa, T.; Vacuum ultraviolet fluorescence spectroscopy of Nd^{3+}:LaF_3 using femtosecond extreme ultraviolet free electron laser, *Appl. Phys. Exp.* **2013**, 6, 022401.

[20] Furukawa, Y.; Cadatal, M.; Yamanoi, K.; Takatori, S.; Pham, M.; Estacio, E.; Nakazato, T.; Shimizu, T.; Sarukura, N.; Kitano, K.; Ando, K.; Uchiyama, K.; Isobe, Y.; Fukuda, K.; Suyama, T.; Yanagida, T.; Yokota, Y.; Yoshikawa, A.; Saito, F. Development of vacuum ultraviolet streak camera system for the evaluation of vacuum ultraviolet emitting materials, *Jpn. J. Appl. Phys.* **2009**, 48, 096503.

[21] Shigemasa, E. UVSOR Activity Report (2010) p. 25. https://www.uvsor.ims.ac.jp/eng/activity/2010/

[22] Perdew, J.P.; Ernzerhof, M.; Burke, K. Rationale for mixing exact exchange with density functional approximations, *J. Chem. Phys*., **1996**, 105, 9982-9985.

[23] Carlo, A.; Barone, V.; Toward reliable density functional methods without adjustable parameters: The PBE0 model, *J. Chem. Phys*., **1999**, 110, 6158-6170.

[24] Aryasetiawandag, F.; Gunnarssonddag, O. The GW method, *Rep. Prog. Phys*., **1998**, 61, 237-312.

[25] García, A.M.; Valero, R.; Illas, F. An empirical, yet practical way to predict the band gap in solids by using density functional band structure calculations, *J. Phys. Chem. C*, **2017,** 121, 18862-18866.

[26] Ziesche, P.; Kurth, S.; Perdew, J.P. Density functionals from LDA to GGA, *Comp. Mater. Sci.,* **1998**, 11, 122-127.

[27] Luong, M.V.; Cadatal-Raduban, M.; Empizo, M.J.F.; Arita, R.; Minami, Y.; Shimizu, T.; Sarukura, N.; Azechi, H.; Pham, M.H.; Nguyen, H.D.; Kawazoe, Y. Comparison of the electronic band structures of $LiCaAlF_6$ and $LiSrAlF_6$ ultraviolet laser host media from ab initio calculations, *Jpn. J. Appl. Phys*., **2015,** 54, 122602.

[28] Luong, M.V.; Empizo, M.J.F.; Gabyano, J.L.F.; Minami, Y.; Yamanoi, K.; Shimizu, T.; Sarukura, N.; Pham, M.H.; Nguyen, H.D.; Steenbergen, K.G.; Schwerdtfeger, P.; Cadatal-Raduban, M. Direct band gap tunability of the $LiYF_4$ crystal through high-pressure applications, *Comp. Mater. Sci.* **2018**, 153, 431-437.

[29] Lv, Z.; Cheng, C.; Cheng, Y.; Chen, X.; Ji, G. Elastic, thermodynamic and electronic properties of LaF_3 under pressure from first principles, *Comp. Mater. Sci.* **2014**, 89, 57-64.

[30] Shimizu, T.; Luong, M.V.; Cadatal-Raduban, M.; Empizo, M.J.F.; Yamanoi, K.; Arita, R.; Minami, Y.; Sarukura, N.; Mitsuo, N.; Azechi, H.; Pham, M.H.; Nguyen, H.D.; Ichiyanagi, K.; Nozawa, S.; Fukaya, R.; Adachi, S.; Nakamura, K.G.; Fukuda, K.; Kawazoe, Y.; Steenbergen, K.G.; Schwerdtfeger, P. High pressure band gap modification of $LiCaAlF_6$ *Appl. Phys. Lett*., **2017,** 110, 141902.